

# $p\bar{\Lambda}$ final-state interaction in the reactions $e^+e^- \rightarrow K^-p\bar{\Lambda}$ and $J/\psi \rightarrow K^-p\bar{\Lambda}$

Johann Haidenbauer<sup>1,a</sup>, Ulf-G. Meißner<sup>2,1,b</sup>

<sup>1</sup>Institute for Advanced Simulation (IAS-4), Forschungszentrum Jülich, D-52428 Jülich, Germany

<sup>2</sup>Helmholtz-Institut für Strahlen- und Kernphysik and Bethe Center for Theoretical Physics, Universität Bonn, D-53115 Bonn, Germany

March 28, 2024

**Abstract** Near-threshold  $p\bar{\Lambda}$  mass spectra for the reactions  $e^+e^- \rightarrow K^-p\bar{\Lambda}$  and  $J/\psi \rightarrow K^-p\bar{\Lambda}$  are investigated with an emphasis on the role played by the interaction in the  $p\bar{\Lambda}$  system. As guideline for the  $p\bar{\Lambda}$  interaction a variety of  $\Lambda\bar{\Lambda}$  potential models is considered that have been established in the analysis of data on  $p\bar{p} \rightarrow \Lambda\bar{\Lambda}$  in the past. Arguments why the properties of the  $p\bar{\Lambda}$  and  $\Lambda\bar{\Lambda}$  interactions can be expected to be very similar are provided. It is shown that the near-threshold enhancement in the invariant mass observed for the  $e^+e^-$  reaction can be reproduced quantitatively by the assumed  $p\bar{\Lambda}$  final-state interaction in the partial wave suggested by an amplitude analysis of the experiment. The effect of the  $p\bar{\Lambda}$  final-state interaction in other decays is explored, including the recently measured reactions  $B^- \rightarrow J/\psi \bar{p}\Lambda$  and  $B^+ \rightarrow J/\psi p\bar{\Lambda}$ . It is found that the final-state interaction improves the description of the measured invariant mass near threshold in most cases.

**Keywords** Hadron production in  $e^+e^-$  interactions ·  $p\bar{\Lambda}$  interaction

**PACS** 13.60.Rj · 13.66.Bc · 14.20.Jn

## 1 Introduction

One of the phenomena that caught a wider attention over the last two decades is the near-threshold enhancement in the invariant mass of baryon-antibaryon ( $B\bar{B}$ ) systems observed in various heavy-meson decays and also in  $e^+e^-$  collisions. The most spectacular example is definitely the anomalously strong enhancement detected in the  $p\bar{p}$  spectrum in the reaction  $J/\psi \rightarrow \gamma p\bar{p}$

[1–3]. Less prominent but still noticeable enhancements as compared to the phase-space behavior have been also observed in other decays like  $J/\psi \rightarrow \pi^0 p\bar{p}$  [1, 4],  $\psi' \rightarrow \gamma p\bar{p}$  [2, 3], and in  $e^+e^- \rightarrow p\bar{p}$  [5, 6]. Reactions with a  $\Lambda\bar{\Lambda}$  system in the final state have been studied, too [7–13] and in this case clear evidence for a near-threshold enhancement has been observed in reactions like  $e^+e^- \rightarrow \eta\Lambda\bar{\Lambda}$  [13] and  $e^+e^- \rightarrow \phi\Lambda\bar{\Lambda}$  [12]. The most puzzling result is definitely the large non-zero cross section barely 1 MeV away from the  $\Lambda\bar{\Lambda}$  threshold, reported in a measurement of the reaction  $e^+e^- \rightarrow \Lambda\bar{\Lambda}$  by the BESIII Collaboration [10].

The two most striking observations mentioned have triggered many studies offering a wide spectrum of possible reasons for the origin of the detected enhancement. Those range from very exotic explanations like glueballs [14–16], or of evidence for new resonances or for  $B\bar{B}$  bound states [1, 3, 17–21], to a more conventional interpretation in form of a final-state interaction (FSI) between the produced  $B\bar{B}$  pair [22–36].

So far, much less attention was paid to the  $p\bar{\Lambda}$  interaction. With the present work we want to provide a remedy of this neglect. Indeed, also for this  $B\bar{B}$  system there is a wealth of data available, though with somewhat less statistics as compared to  $p\bar{p}$  and/or  $\Lambda\bar{\Lambda}$ , and a near-threshold enhancement has been observed in some reactions. To be concrete, there are measurements of the  $p\bar{\Lambda}$  ( $p\bar{\Lambda}$ ) invariant mass spectrum near the threshold in the reactions  $J/\psi \rightarrow K^-p\bar{\Lambda}$  and  $\psi(3686) \rightarrow K^-p\bar{\Lambda}$  by the BES Collaboration [37], and for  $\chi_{c0} \rightarrow K^+\bar{p}\Lambda$  [38],  $\psi(3686) \rightarrow K^{*+}\bar{p}\Lambda$  [39], and  $e^+e^- \rightarrow K^-p\bar{\Lambda}$  [40] by BESIII<sup>1</sup>. From the enhancement seen in  $J/\psi \rightarrow K^-p\bar{\Lambda}$  the resonance parameters  $m = 2075 \pm 12 \pm$

<sup>1</sup>Note that in experiments with neutral initial states like  $J/\psi$  or  $e^+e^-$  usually the data for the two charge-conjugated decay modes are combined, e.g. those for  $K^-p\bar{\Lambda}$  and  $K^+\bar{p}\Lambda$ . Thus,

<sup>a</sup>e-mail: j.haidenbauer@fz-juelich.de

<sup>b</sup>e-mail: meissner@hiskp.uni-bonn.de

5 MeV,  $\Gamma = 90 \pm 35$  MeV (assuming an  $S$ -wave) or  $m = 2044 \pm 17$  MeV,  $\Gamma = 20 \pm 45$  MeV ( $P$ -wave) have been deduced [37]. In case of  $e^+e^- \rightarrow K^- p\bar{\Lambda}$  an amplitude analysis has been performed and the enhancement was attributed to the  $1^+$  ( $P$ -wave) state. Here the reported parameters are  $m = 2084_{-2}^{+4} \pm 9$  MeV,  $\Gamma = 58_{-3}^{+4} \pm 25$  MeV [40]. A fit to the enhancement observed in  $\chi_{c0} \rightarrow K^+ \bar{p}\bar{\Lambda}$  yielded  $m = 2053 \pm 13$  MeV,  $\Gamma = 292 \pm 14$  MeV, with preference for  $0^-$  ( $^1S_0$  state) [38]. However, in all aforementioned experiments there is no distinct peak-like structure in the measured spectrum and the deduced resonances overlap with the threshold (within their width) or even lie below the  $p\bar{\Lambda}$  threshold, which is at 2053.95 MeV. Thus, using a Breit-Wigner type ansatz is incorrect, as the underlying assumption of a slowly varying background is certainly not fulfilled in the vicinity of a threshold.

There are also measurements for  $J/\psi \rightarrow K_S^0 n\bar{\Lambda}$  [41] and the decays  $\chi_{cJ} \rightarrow K_S^0 n\bar{\Lambda}$  for  $J = 0, 1, 2$  [42]. In addition there are preliminary data by the GlueX Collaboration on  $\gamma p \rightarrow \Lambda\bar{\Lambda}p$  [43, 44]. Finally, measurements of the  $p\bar{\Lambda}$  ( $p\bar{\Lambda}$ ) invariant mass have been reported for  $B^0 \rightarrow \pi^- p\bar{\Lambda}$  by the Belle [45] and BaBar [46] Collaborations, and for the reactions  $B^- \rightarrow J/\psi \bar{p}\bar{\Lambda}$  [47, 48] and  $B^+ \rightarrow J/\psi p\bar{\Lambda}$  [49].

In the present work we want to review and re-examine the information on the  $p\bar{\Lambda}$  interaction. In particular, we want to investigate to what extent the FSI between these two baryons plays a role in understanding and interpreting their invariant-mass spectrum in the near-threshold region. The main focus will be certainly on the decay of  $J/\psi$  and the signal in  $e^+e^-$  collisions, where evidence for resonances has been claimed as mentioned above. However, we will also explore the situation for several other reactions where near-threshold results for the  $p\bar{\Lambda}$  spectrum have been published.

Without ready access to a suitable  $p\bar{\Lambda}$  potential, as guide line for the momentum dependence of the  $p\bar{\Lambda}$  FSI a variety of  $\Lambda\bar{\Lambda}$  potential models is utilized that have been established in the analysis of data on  $p\bar{p} \rightarrow \Lambda\bar{\Lambda}$  [50] in the past [51, 52]. Arguments why the properties of the  $p\bar{\Lambda}$  and  $\Lambda\bar{\Lambda}$  interactions can be expected to be very similar are provided below. One of those are measurements of two-particle correlation functions in heavy-ion collisions [53, 54] by the STAR Collaboration (in Au-Au collisions at  $\sqrt{s_{NN}} = 200$  GeV) and in high-energy  $pp$  collisions by the ALICE Collaboration [55, 56] which yielded very similar results for  $p\bar{\Lambda}$  and  $\Lambda\bar{\Lambda}$ .

The paper is structured in the following way. In the subsequent section we provide a brief summary of the employed formalism for treating the FSI effects. In

throughout our paper we will not distinguish between  $p\bar{\Lambda}$  and  $\bar{p}\Lambda$ .

Sect. 3 we present our results. Specifically, we investigate the  $p\bar{\Lambda}$  FSI for  $e^+e^- \rightarrow K^- p\bar{\Lambda}$  and  $J/\psi \rightarrow K^- p\bar{\Lambda}$  and then show our predictions for the  $p\bar{\Lambda}$  invariant mass spectra measured in the reactions  $B^- \rightarrow J/\psi \bar{p}\bar{\Lambda}$  and  $B^+ \rightarrow J/\psi p\bar{\Lambda}$ . We also discuss the situation for  $\psi(3868) \rightarrow K^- p\bar{\Lambda}$  and  $\chi_{cJ} \rightarrow K^- p\bar{\Lambda}$  among others. The paper closes with a short summary.

## 2 Treatment of the $B\bar{B}$ final-state interaction

How we treat the FSI is described and discussed in detail in Refs. [23, 29, 35]. Thus, below we provide only a summary of the essential formulae. The calculation of the  $B\bar{B}$  invariant-mass spectrum is based on the distorted wave Born approximation (DWBA), where the reaction amplitude  $A$  is given schematically by [23, 29]

$$A = A^0 + A^0 G^{B\bar{B}} T^{B\bar{B}}. \quad (1)$$

Here,  $A^0$  is the elementary (or primary) production amplitude,  $G^{B\bar{B}}$  the free  $B\bar{B}$  Green's function, and  $T^{B\bar{B}}$  the  $B\bar{B}$  reaction amplitude. The explicit expression for a specific partial wave with orbital angular momentum  $L$  reads

$$A_L(k) = \bar{A}_L^0 k^L \times \left[ 1 + \int_0^\infty \frac{dpp^2}{(2\pi)^3} \frac{p^L}{k^L} \frac{1}{\sqrt{s} - E_p + i0^+} T_L(p, k; \sqrt{s}) \right], \quad (2)$$

with  $\sqrt{s} = M_{B\bar{B}} = \sqrt{m_{B_1}^2 + k^2} + \sqrt{m_{B_2}^2 + k^2}$  the  $B\bar{B}$  invariant mass (energy in the  $B\bar{B}$  subsystem) and  $E_p = \sqrt{m_{B_1}^2 + p^2} + \sqrt{m_{B_2}^2 + p^2}$ . The momentum factor  $k^L$  is pulled out so that  $\bar{A}_L^0$  is essentially a constant near threshold (see the detailed discussion in [35]). The  $B\bar{B}$   $T$ -matrix,  $T_L(p, k; \sqrt{s})$ , is obtained by solving the Lippmann-Schwinger (LS) equation,

$$T_L(p', k; \sqrt{s}) = V_L(p', k) + \int_0^\infty \frac{dpp^2}{(2\pi)^3} V_L(p', p) \frac{1}{\sqrt{s} - E_p + i0^+} T_L(p, k; \sqrt{s}), \quad (3)$$

for a specific  $B\bar{B}$  potential  $V_L$ . In the case of coupled partial waves like the  $^3S_1$ - $^3D_1$  the corresponding coupled LS equation is solved [31], and then  $T_{LL}$  is used in Eq. (2).

The  $p\bar{\Lambda}$  invariant-mass spectrum is calculated via

$$\frac{d\sigma}{dM} \propto k |A_L(k)|^2, \quad (4)$$

which is valid when the (total) energy is significantly larger than the  $K^- p\bar{\Lambda}$  threshold energy. Then for low  $p\bar{\Lambda}$  invariant masses the relative momentum of the third particle is large and its interaction does not distort the

signal of interest. This condition is fulfilled by most of the reactions where measurements by the BESIII Collaboration are available. In cases like  $B^+ \rightarrow J/\psi p\bar{\Lambda}$  where the available phase space is small we evaluate the three-particle phase space explicitly [57],

$$\frac{d\sigma}{dM} \propto \lambda^{1/2}(s_{\text{tot}}, M^2, m_K^2) \lambda^{1/2}(M^2, m_p^2, m_\Lambda^2) |A_L(k)|^2, \quad (5)$$

where the Källén function  $\lambda$  is defined by  $\lambda(x, y, z) = ((x - y - z)^2 - 4yz)/4x$ ,  $M \equiv M_{p\bar{\Lambda}}$  is the invariant mass of the  $p\bar{\Lambda}$  system and  $s_{\text{tot}}$  is the total energy squared.

The results shown below are based on the  $\Lambda\bar{\Lambda}$  potentials used in our analysis of the reactions  $e^+e^- \rightarrow \phi\Lambda\bar{\Lambda}$  and  $e^+e^- \rightarrow \eta\Lambda\bar{\Lambda}$  [35]. Indeed, there is an almost complete lack of  $p\bar{\Lambda}$  potentials [58], among other reasons because there is no extensive empirical information that would allow to establish such an interaction, quite in contrast to  $\Lambda\bar{\Lambda}$  which can be reasonably well constrained by data on the reaction  $p\bar{p} \rightarrow \Lambda\bar{\Lambda}$ , for which differential cross sections, polarizations, etc. have been measured down to energies very close to the threshold [50]. The employed  $\Lambda\bar{\Lambda}$  potentials (I-IV) are described in detail in Refs. [51, 52], see also the discussion in [35]. They consist of an elastic part generated by meson exchanges, and an annihilation part in form of a phenomenological optical potential. As already said above, all of them have been determined in a fit to the wealth of  $p\bar{p} \rightarrow \Lambda\bar{\Lambda}$  data collected by the P185 Collaboration [50].

We decided to employ those  $\Lambda\bar{\Lambda}$  potentials for generating the FSI effects because first exploratory calculations with them yielded quite promising results for the measured  $p\bar{\Lambda}$  spectra. Anyway, it can be expected that the interactions in the  $B\bar{B}$  systems exhibit some universal properties which are essential for reproducing the threshold behavior of the invariant-mass spectrum. The most important aspect is that annihilation processes dominate the  $\Lambda\bar{\Lambda}$  as well as the  $p\bar{\Lambda}$  interactions. Furthermore, in both cases one-pion exchange is not possible, and thus there is no long-range elastic contribution. Finally, in both cases there is only one isospin state, so that no near-threshold coupling, say, like that between  $p\bar{p}$  and  $n\bar{n}$ , exists. Taking those aspects together, it is a reasonable working hypothesis to assume that the properties of the FSI effects due to the  $\Lambda\bar{\Lambda}$  and  $p\bar{\Lambda}$  interactions are very similar.

It should be added that the similarity of the  $\Lambda\bar{\Lambda}$  and  $p\bar{\Lambda}$  interactions is supported by measurements of the pertinent correlation functions. Available data from the STAR and ALICE Collaborations demonstrate that the momentum dependence established for the two systems

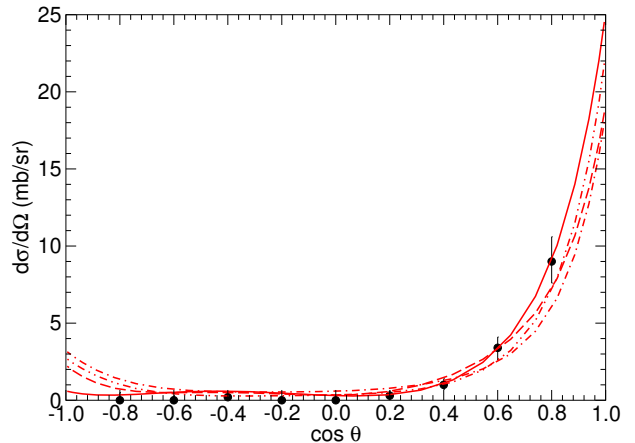


**Fig. 1** Differential cross section for  $p\bar{\Lambda}$  scattering at  $p_{\text{lab}} = 1.074 \pm 0.017$  GeV [59]. The curves are predictions by the  $\Lambda\bar{\Lambda}$  interactions I-IV, see Ref. [35], at 1.05 GeV/c.

is practically the same [53–56]. Interestingly, even observables like the differential cross section could be similar, as suggested by the comparison of a recent measurement of  $p\bar{\Lambda}$  scattering at roughly 1 GeV by BESIII [59] with a prediction for  $\Lambda\bar{\Lambda}$  employing the phenomenological potentials published by the Jülich Group [51, 52], see Fig. 1. Though, in principle, one cannot exclude that this agreement is purely accidental, very likely it is an indication that both interactions are really dominated by strong and universal annihilation processes, as already argued in [59].

In principle, one could try to construct a phenomenological  $p\bar{\Lambda}$  potential. But in view of the semi-quantitative agreement of the  $\Lambda\bar{\Lambda}$  results with the  $p\bar{\Lambda}$  data (after adjusting for phase-space differences), to be reported below, one would anyway adopt the  $\Lambda\bar{\Lambda}$  potential as determined in the fit to the  $p\bar{p} \rightarrow \Lambda\bar{\Lambda}$  data as starting point. In fact, by recalling the Schrödinger equation,

$$-u''(k, r) + 2\mu_{B_1 B_2} V_{B_1 B_2}(r) u(k, r) = k^2 u(k, r),$$

with  $u(k, r)$  the wave function and  $\mu_{B_1 B_2}$  the reduced mass, obtaining an  $p\bar{\Lambda}$  potential can be simply realized by requiring that  $\mu_{p\bar{\Lambda}} V_{p\bar{\Lambda}} \simeq \mu_{\Lambda\bar{\Lambda}} V_{\Lambda\bar{\Lambda}}$ . Then the  $k$  dependence of all observables, including the mass spectrum for the  $p\bar{\Lambda}$  and  $\Lambda\bar{\Lambda}$  systems would be identical. The ratio of the reduced masses is 1.09 so that the  $p\bar{\Lambda}$  potential established that way would be about 10 % stronger than that for  $\Lambda\bar{\Lambda}$ .

Since there are no  $C$ -parity restrictions in reactions involving the  $K$  meson, the selection rules for the decay to the  $Kp\bar{\Lambda}$  final state are less rigid and, in general,

**Table 1** Allowed  $p\bar{\Lambda}$  partial waves ( $^{2S+1}L_J$ ) and  $J^P$  assignments (up to  $P$ -waves) for various initial states.  $s, p, d$  indicate the relative orbital angular momentum of the  $K$  meson.

initial state	partial waves
$J/\psi[1^-]$	$^1S_0p[0^-], ^3S_1p[1^-], ^1,^3P_1s[1^+], ^3P_2d[2^+]$
$e^+e^-[1^-]$	$^1S_0p[0^-], ^3S_1p[1^-], ^1,^3P_1s[1^+], ^3P_2d[2^+]$
$\chi_{c0}[0^+]$	$^1S_0s[0^-], ^1,^3P_1p[1^+]$
$\chi_{c1}[1^+]$	$^3S_1s[1^-], ^1,^3P_1p[1^+], ^3P_2p[2^+]$
$\chi_{c2}[2^+]$	$^1S_0d[0^-], ^3S_1d[1^-], ^1,^3P_1p[1^+], ^3P_2p[2^+]$

both spin states of the  $p\bar{\Lambda}$  ( $\bar{p}\Lambda$ ) system can occur. An overview of the allowed partial waves is given in Tab. 1.

### 3 Results

In the following we explore the  $p\bar{\Lambda}$  invariant-mass spectrum as measured in various heavy-meson decays and in  $e^+e^-$ . We start with the reactions  $e^+e^- \rightarrow K^-p\bar{\Lambda}$  and  $J/\psi \rightarrow K^-p\bar{\Lambda}$  where data are available from the BES [37] and BESIII [40] Collaborations and where evidence for a narrow structure near the  $p\bar{\Lambda}$  threshold has been claimed [40]. Then we take a look at  $B^+ \rightarrow J/\psi p\bar{\Lambda}$  and  $B^- \rightarrow J/\psi \bar{p}\Lambda$ , where the CMS [49] and LHCb [48] Collaborations provided invariant-mass spectra with excellent momentum resolution and where in the latter measurement evidence for a pentaquark, the  $P_{\psi_s}^{\Lambda}(4338)$ , has been reported. Finally, we illustrate the situation for other reactions where results for the  $p\bar{\Lambda}$  or  $n\bar{\Lambda}$  invariant mass have been presented, although with lower resolution. As mentioned above, the present investigation exploits the momentum dependence predicted by the  $\Lambda\bar{\Lambda}$  potentials from [51, 52] which has been already examined in the study of the electromagnetic form factors of the  $\Lambda$  in the time-like region [32] and in various meson decays with  $\Lambda\bar{\Lambda}$  in the final state [35].

As a reminder, and as already emphasized in Refs. [29, 35] the validity of treating FSI effects via Eqs. (2) and (4) is clearly limited, say to excess energies of 50 to 100 MeV. With increasing invariant mass the momentum dependence of the reaction/production mechanism should become more and more relevant and will likewise influence the invariant-mass spectrum.

Note further that for none of the measurements considered below the data have been published in numerical form. Thus, we digitized them from the pertinent figures.

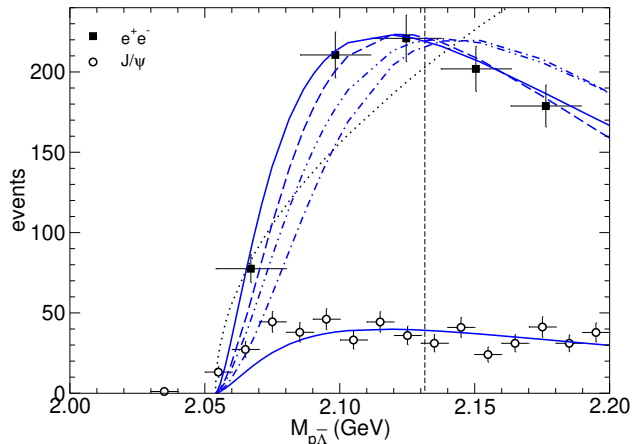


**Fig. 2** Invariant-mass spectra for  $e^+e^- \rightarrow K^-p\bar{\Lambda}$  (open squares) [40] and  $J/\psi \rightarrow K^-p\bar{\Lambda}$  (black) [37] (filled circles). The bin width for the former is 26 MeV, while for the latter it is 10 MeV. Blue curves are based on the momentum dependence predicted by the  $\Lambda\bar{\Lambda}$  interaction I-IV [35] in the  $^3P_1$  partial wave, corresponding to the quantum number  $J^P = 1^+$  of the resonance proposed by BESIII. The phase-space behavior is indicated by the dotted line. The vertical dashed line marks the  $p\bar{\Lambda}$  threshold.

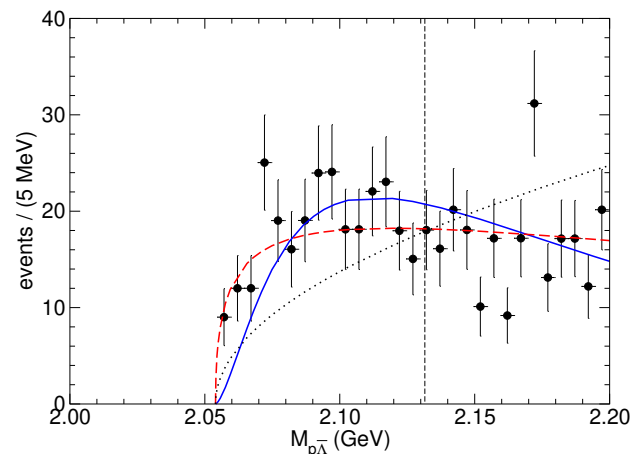


**Fig. 3** Invariant-mass spectrum for  $J/\psi \rightarrow K^-p\bar{\Lambda}$  [37]. The solid (blue) curve is based on the  $\Lambda\bar{\Lambda}$  interaction I [35] in the  $^3P_1$  partial wave while the dashed (red) curve is based on the  $^3S_1$  partial wave.

#### 3.1 The reactions $e^+e^- \rightarrow K^-p\bar{\Lambda}$ and $J/\psi \rightarrow K^-p\bar{\Lambda}$

In a recent paper the BESIII Collaboration reported evidence for a narrow structure in the  $p\bar{\Lambda}$  system near threshold from a measurement of  $e^+e^- \rightarrow K^-p\bar{\Lambda}$  [40]. The spin and parity of the structure was determined to be  $J^P = 1^+$  and the values  $m = 2084_{-2}^{+4} \pm 9$  MeV,

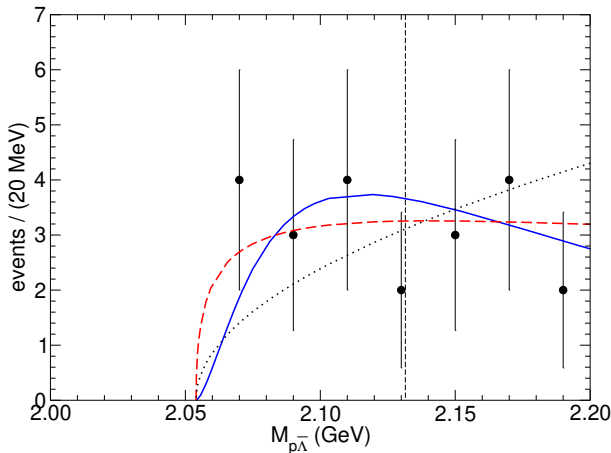


**Fig. 4** Invariant-mass spectrum for  $\psi(3686) \rightarrow K^- p\bar{\Lambda}$  [37]. Same description of curves as in Fig. 3.

$\Gamma = 58_{-3}^{+4} \pm 25$  MeV for its pole position were extracted from a fit to the line shape with a relativistic Breit-Wigner function. We point out that doing this so close to threshold is not appropriate. Already in 2004 the BES Collaboration had measured the reaction  $J/\psi \rightarrow K^- p\bar{\Lambda}$  [37] and an enhancement of the near-threshold  $p\bar{\Lambda}$  invariant mass had been detected which could be fitted by a resonance with parameters  $m = 2075 \pm 12 \pm 5$  MeV,  $\Gamma = 90 \pm 35$  MeV (assuming an  $S$ -wave) or  $m = 2044 \pm 17$  MeV,  $\Gamma = 20 \pm 45$  MeV ( $P$ -wave).

Since the  $p\bar{\Lambda}$  ( $p\bar{\Lambda}$ ) threshold is at 2053.95 MeV it is obvious that those resonances overlap with the threshold region, considering their width. In such a case it is practically impossible to disentangle resonance effects from an ordinary FSI. Therefore, it is tempting to explore whether a possible FSI in the  $p\bar{\Lambda}$  system could also explain the enhancement seen in the experiment. Assuming the spin and parity determined by BESIII, the  $p\bar{\Lambda}$  interaction should take place dominantly in the  ${}^3P_1$  (or  ${}^1P_1$ ) partial wave. Corresponding results are shown in Fig. 2 based on the momentum dependence of the  $\Lambda\bar{\Lambda}$  models I-IV [51, 52] employed in our study of the  $\Lambda\bar{\Lambda}$  FSI [35]. In order to guide the eye we show the phase space behavior (dotted line), arbitrarily normalized to the data at an excess energy of  $\sim 90$  MeV. Furthermore we indicate the  $p\bar{\Sigma}$  threshold by a vertical line. Actually, neither the  $p\bar{\Lambda}$  ( $p\bar{\Lambda}$ ) correlation functions nor the considered data on the  $p\bar{\Lambda}$  ( $p\bar{\Lambda}$ ) spectra do show any convincing evidence for the opening of the  $p\bar{\Sigma}$  ( $p\bar{\Sigma}$ ) threshold which is around  $M_{p\bar{\Lambda}} = 2.131$  GeV. This is quite different from the  $p\bar{\Lambda}$  system where a sizable cusp at the  $p\bar{\Sigma}$  has been seen in many experiments [60, 61]. We see that as further justification for the simplified

treatment of the  $p\bar{\Lambda}$  ( $p\bar{\Lambda}$ ) interaction in the present work.

Obviously, and not unexpectedly, there is a sizable model dependence of the predicted invariant-mass spectrum. But all results show the same qualitative trend, namely an enhancement of the invariant mass near threshold. Moreover, intriguingly two of the model yield results that are quite well in line with the experiment. Specifically, model I (solid line) reproduces the near-threshold behavior of the  $p\bar{\Lambda}$  invariant mass from the BESIII experiment  $e^+e^- \rightarrow K^- p\bar{\Lambda}$  [40] (open squares) more or less exactly. Since the momentum dependence predicted by that model is so clearly favored by the data we select it as basis for the subsequent discussion.

In the same figure, one can find also results for the  $p\bar{\Lambda}$  spectrum deduced from the reaction  $J/\psi \rightarrow K^- p\bar{\Lambda}$  [37] (filled circles), again confronted with theory. With regard to the latter we show only the prediction based on model I for reasons of clarity. Also in this case the FSI reproduces the overall trend of the invariant-mass spectrum quite well, though there might be a discrepancy very close to threshold. In order to shed light on that region, in Fig. 3 we compare our results with  $p\bar{\Lambda}$  data with refined binning, cf. Fig. 2(c) in [37]. In addition, we include predictions based on the  ${}^3S_1$  partial wave of model I (dashed red line). Obviously both scenarios are well in line with the experiment, given the present uncertainties.

Finally, in Ref. [37] results for the  $p\bar{\Lambda}$  invariant-mass spectrum from  $\psi(3686) \rightarrow K^- p\bar{\Lambda}$  were presented. Those are shown in Fig. 4, again in comparison to predictions. For that reaction the statistics is much lower. But still there is clear evidence for a deviation from the phase-space behavior [37] and strong support for the presence of a FSI, which could be either in the  ${}^3P_1$  or  ${}^3S_1$ .

### 3.2 The reactions $B^+ \rightarrow J/\psi p\bar{\Lambda}$ and $B^- \rightarrow J/\psi \bar{p}\Lambda$

In Figs. 5 and 6 we present the  $p\bar{\Lambda}$  ( $\bar{p}\Lambda$ ) invariant-mass spectrum measured in the reactions  $B^+ \rightarrow J/\psi p\bar{\Lambda}$  and  $B^- \rightarrow J/\psi \bar{p}\Lambda$  by the CMS [49] and LHCb [48] Collaborations, respectively. Those data are very interesting because of the excellent invariant-mass resolution. However, there is also a caveat. The available phase space is with less than 130 MeV extremely small so that the interactions in the other two-body final states ( $J/\psi p$ ,  $J/\psi \bar{p}$ ,  $J/\psi \Lambda$ ) could already distort the signal of the  $p\bar{\Lambda}$  ( $\bar{p}\Lambda$ ) interaction and then Eqs. (2) are no longer applicable. One should keep that in mind. In any case, the region for realistic conclusions is certainly restricted to, say, 20 to 30 MeV from the threshold. Given that restrictions it is really remarkable that the

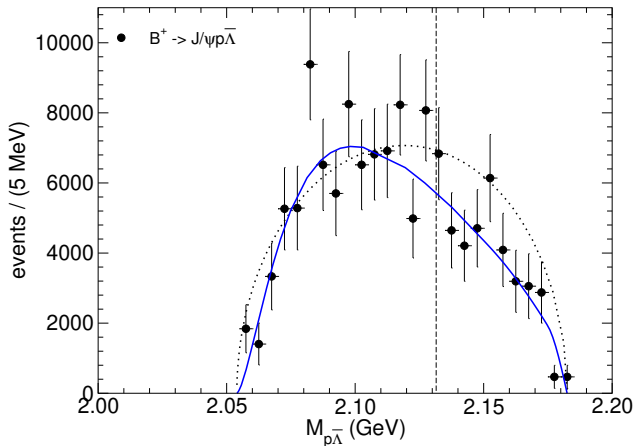


**Fig. 5** Invariant-mass spectrum for  $B^+ \rightarrow J/\psi p\bar{\Lambda}$  from CMS [49], The blue curve is based on the  $\Lambda\bar{\Lambda}$  interaction in the  $^3P_1$  partial wave. Same description of curves as in Fig. 3.

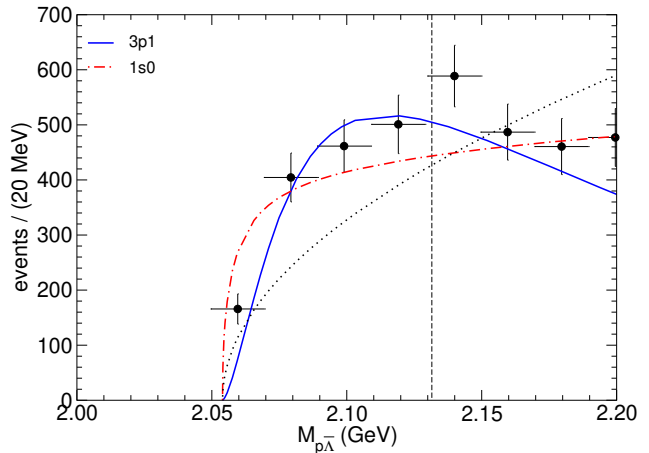


**Fig. 7** Invariant-mass spectrum for  $\chi_{c0} \rightarrow K^+ \bar{p}\Lambda$  [38]. The solid (blue) curve is based on the  $\Lambda\bar{\Lambda}$  interaction in the  $^3P_1$  partial wave while the dashed-dotted (red) curve is based on the  $^1S_0$  partial wave.

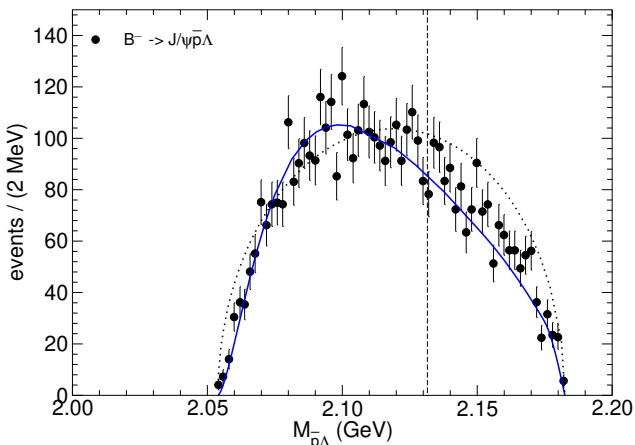


**Fig. 6** Invariant-mass spectrum for  $B^- \rightarrow J/\psi \bar{p}\Lambda$  from LHCb [48], The blue curve is based on the  $\Lambda\bar{\Lambda}$  interaction in the  $^3P_1$  partial wave. Same description of curves as in Fig. 3.

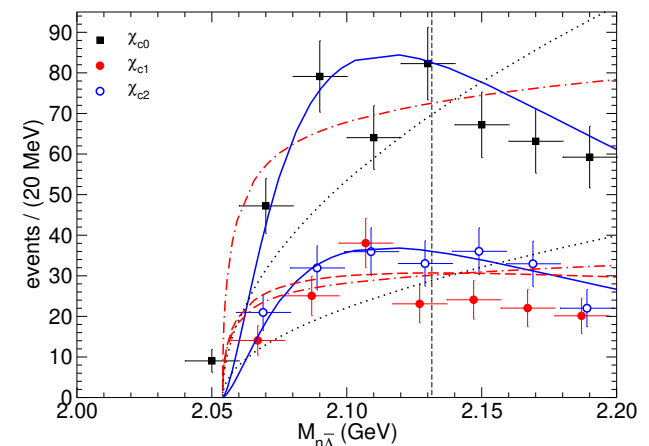


**Fig. 8** Invariant-mass spectrum for  $\chi_{cJ} \rightarrow K_S^0 \bar{n}\Lambda$  ( $J = 0, 1, 2$ ) [42]. Same description of curves as in Figs. 3 and 7.

data follow very closely the predictions based on the  $^3P_1$  partial wave near the threshold, see Figs. 5, 6. We see that as clear signature that the  $1^+$  dominates here, and not the  $1^-$  [48]. Interestingly, with the  $p\bar{\Lambda}$  ( $\bar{p}\Lambda$ ) interaction in the  $^3P_1$  the invariant mass over the whole phase space is described rather well, when the phase-space factor Eq. (5) is appropriately taken into account.

### 3.3 The $p\bar{\Lambda}$ invariant-mass spectrum in other reactions

In Figs. 7 - 11 we show result for other reactions where the  $p\bar{\Lambda}$  invariant-mass spectrum has been measured.

Also in those cases, in general we assume that either the  $^3S_1$  or the  $^3P_1$  partial waves provide the dominant FSI effect. An exception is the  $\chi_{c0}$  decay, where the  $^3S_1$  is not allowed, only the  $^1S_0$ , see Tab. 1.

Let us start with  $\chi_{cJ}$  decays where data are available from the reactions  $\chi_{c0} \rightarrow K^+ \bar{p}\Lambda$  [38] and  $\chi_{cJ} \rightarrow K_S^0 \bar{n}\Lambda$  ( $J = 0, 1, 2$ ) [42] (Figs. 7 and 8). In all cases the measured  $N\bar{\Lambda}$  spectra are quite well in line with a FSI dominated by the  $^3P_1$  partial wave. In this context let us mention that the BESIII Collaboration has deduced a resonance in the  $^1S_0$  ( $0^-$ ) partial wave from those data on  $\chi_{c0} \rightarrow K^+ \bar{p}\Lambda$  [38] with the properties

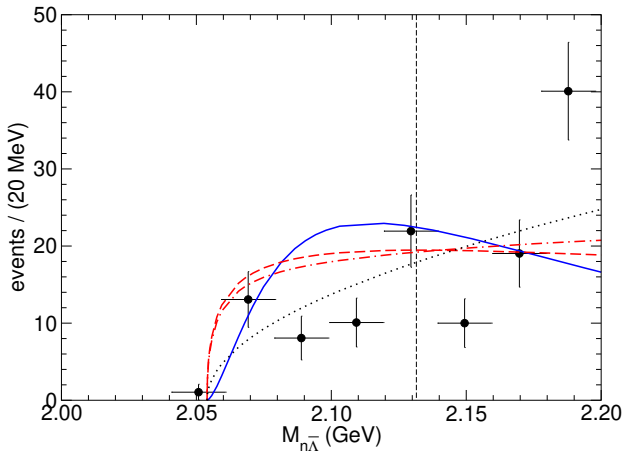


**Fig. 9** Invariant-mass spectrum for  $J/\psi \rightarrow K_S^0 \bar{n} \Lambda$  [41]. Same description of curves as in Figs. 3 and 7.

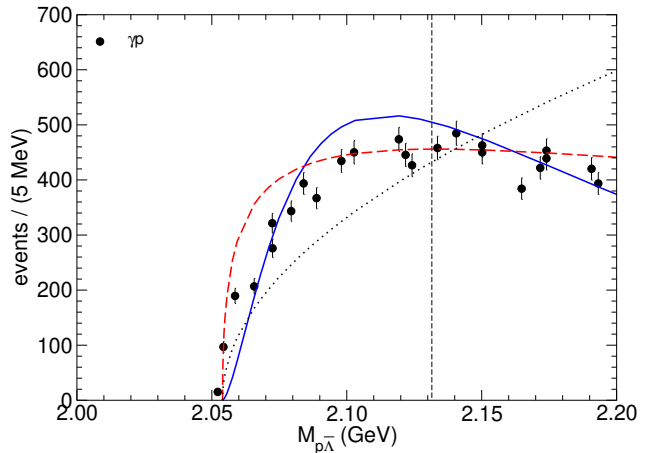


**Fig. 11** Invariant-mass spectrum for  $\gamma p \rightarrow \Lambda \bar{p}$ . The red squares are preliminary data from a GlueX experiment [43]. Same description of curves as in Fig. 3.

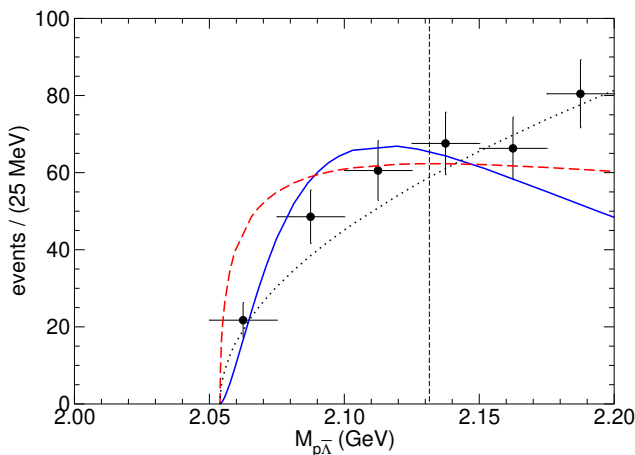


**Fig. 10** Invariant-mass spectrum for  $\psi(3686) \rightarrow K^{*+} \bar{p} \Lambda$  [39]. Same description of curves as in Fig. 3.

$m = 2053 \pm 13$  MeV,  $\Gamma = 292 \pm 14$  MeV. In Ref. [62] an explanation of the near-threshold enhancement is given in terms of a tree-level calculation that includes contributions from the intermediate  $K(1830)$ ,  $N(2300)$  and  $\Lambda(1520)$  resonances.

The  $n\bar{\Lambda}$  final state has been also measured in  $J/\psi \rightarrow K_S^0 \bar{n} \Lambda$  [41] (Fig. 9). However, in this case conclusions are difficult to draw. The same applies to data on  $\psi(3686) \rightarrow K^{*+} \bar{p} \Lambda$  [39], shown in Fig. 10, which are, in principle, even consistent with the phase-space behavior.

Finally, there is a measurement of the  $p\bar{\Lambda}$  invariant-mass spectrum from the reaction  $\gamma p \rightarrow p \Lambda \bar{\Lambda}$  by the GlueX Collaboration [43]. As one can see from Fig. 11,

those data are likewise roughly in line with our prediction based on the FSI in the  $^3P_1$  partial wave. However, we want to emphasize that the results are still preliminary. Moreover, the small bin width in combination with the scale of the figure in Ref. [43] prevents a very reliable extraction of the actual values.

Further measurements of the  $p\bar{\Lambda}$  ( $p\bar{\Lambda}$ ) invariant mass have been reported for  $B^0 \rightarrow \pi^- p\bar{\Lambda}$  by the Belle [45] and BaBar [46] Collaborations, but in these cases the bin width is 200 MeV or more so that possible near-threshold FSI effects cannot be resolved. Therefore, we do not consider those data in the present work.

#### 4 Summary and conclusions

In the present work we have investigated invariant-mass spectra for the reactions  $e^+e^- \rightarrow K^- p\bar{\Lambda}$  and  $J/\psi \rightarrow K^- p\bar{\Lambda}$  close to the  $p\bar{\Lambda}$  threshold. Specific emphasis has been put on the effect of the interaction between the final baryon-antibaryon pair which is taken into account rigorously. For it, as a working hypothesis and as guide line, a variety of  $\Lambda\bar{\Lambda}$  potential models have been utilized. Those potentials, established in the analysis of data on the reaction  $p\bar{p} \rightarrow \Lambda\bar{\Lambda}$  from the LEAR facility at CERN, had been already successfully applied in our analysis of FSI effects in the reactions  $e^+e^- \rightarrow \Lambda\bar{\Lambda}$ ,  $e^+e^- \rightarrow \eta\Lambda\bar{\Lambda}$ , and  $e^+e^- \rightarrow \phi\Lambda\bar{\Lambda}$  [35].

It turned out that the near-threshold invariant-mass dependence of the  $p\bar{\Lambda}$  spectra observed in those two reactions can be well reproduced by considering the  $p\bar{\Lambda}$  FSI. Specifically, the data for the reaction  $e^+e^- \rightarrow K^- p\bar{\Lambda}$  can be perfectly described with an FSI in the

partial wave suggested by the amplitude analysis of the experiment. The high-precision measurements for the reactions  $B^+ \rightarrow J/\psi p\bar{\Lambda}$  and  $B^- \rightarrow J/\psi \bar{p}\Lambda$  show also clear evidence for FSI in the  $p\bar{\Lambda}$  ( $\bar{p}\Lambda$ )  $1^+$  state. Regarding the empirical information for other reactions our study is less conclusive, not least because in most cases the statistics of the experiments is significantly lower.

As already concluded from other investigations in the past, there is strong evidence that the final-state interaction in baryon-antibaryon systems can and certainly does influence the properties of the invariant-mass spectrum in the near-threshold region. It has to be taken into account in any serious study that aims at a quantitative analysis of the threshold region. If this is not done, any noticeable deviation from the pure phase-space behavior will be automatically attributed to near- or sub-threshold resonances. Allowing for the presence of FSI effects is the only way to avoid misinterpretations.

**Acknowledgements:** Work supported by the European Research Council (ERC) under the European Union’s Horizon 2020 research and innovation programme (grant no. 101018170, EXOTIC), and by the DFG and the NSFC through funds provided to the Sino-German CRC 110 “Symmetries and the Emergence of Structure in QCD” (Project number 196253076 - TRR 110). The work of UGM was also supported by the Chinese Academy of Sciences (CAS) through a President’s International Fellowship Initiative (PIFI) (Grant No. 2018DM0034).

## References

1. J. Z. Bai *et al.* [BES], Phys. Rev. Lett. **91**, 022001 (2003).
2. J. P. Alexander *et al.* [CLEO], Phys. Rev. D **82**, 092002 (2010).
3. M. Ablikim *et al.* [BESIII], Phys. Rev. Lett. **108**, 112003 (2012).
4. M. Ablikim *et al.* [BES], Phys. Rev. D **80**, 052004 (2009).
5. J.P. Lees *et al.*, Phys. Rev. D **87**, 092005 (2013).
6. R. R. Akhmetshin *et al.* [CMD-3], Phys. Lett. B **794**, 64 (2019).
7. M. Ablikim *et al.* [BESIII], Phys. Rev. D **106**, 072006 (2022).
8. M. Ablikim *et al.* [BESIII], Phys. Rev. D **87**, 052007 (2013).
9. B. Aubert *et al.* [BaBar Collaboration], Phys. Rev. D **76**, 092006 (2007).
10. M. Ablikim *et al.* [BESIII], Phys. Rev. D **97**, 032013 (2018).
11. M. Ablikim *et al.* [BESIII], Phys. Rev. D **107**, 072005 (2023).
12. M. Ablikim *et al.* [BESIII], Phys. Rev. D **104**, 052006 (2021).
13. M. Ablikim *et al.* [BESIII], [arXiv:2211.10755 [hep-ex]].
14. N. Kochelev and D. P. Min, Phys. Lett. B **633**, 283 (2006).
15. B. A. Li, Phys. Rev. D **74**, 034019 (2006).
16. X. G. He, X. Q. Li, X. Liu and J. P. Ma, Eur. Phys. J. C **49**, 731 (2007).
17. A. Datta and P. J. O’Donnell, Phys. Lett. B **567**, 273 (2003).
18. G. J. Ding and M. L. Yan, Phys. Rev. C **72**, 015208 (2005).
19. M. L. Yan, S. Li, B. Wu and B.-Q. Ma, Phys. Rev. D **72**, 034027 (2005).
20. X. Cao, J.-P. Dai and Y.-P. Xie, Phys. Rev. D **98**, 094006 (2018).
21. Z. Y. Li, A. X. Dai and J. J. Xie, Chin. Phys. Lett. **39**, 011201 (2022).
22. B. Kerbikov, A. Stavinsky and V. Fedotov, Phys. Rev. C **69**, 055205 (2004).
23. A. Sibirtsev, J. Haidenbauer, S. Krewald, U.-G. Meißner and A. W. Thomas, Phys. Rev. D **71**, 054010 (2005).
24. J. Haidenbauer, U.-G. Meißner and A. Sibirtsev, Phys. Rev. D **74**, 017501 (2006).
25. B. Loiseau and S. Wycech, Phys. Rev. C **72**, 011001 (2005).
26. D. R. Entem and F. Fernandez, Phys. Rev. D **75**, 014004 (2007).
27. J.-P. Dedonder, B. Loiseau, B. El-Bennich and S. Wycech, Phys. Rev. C **80**, 045207 (2009).
28. G.-Y. Chen, H.R. Dong and J.P. Ma, Phys. Lett. B **692**, 136 (2010).
29. X. W. Kang, J. Haidenbauer and U.-G. Meißner, Phys. Rev. D **91**, 074003 (2015).
30. A. I. Milstein and S. G. Salnikov, Nucl. Phys. A **966**, 54 (2017).
31. J. Haidenbauer, X. W. Kang and U.-G. Meißner, Nucl. Phys. A **929**, 102 (2014).
32. J. Haidenbauer and U.-G. Meißner, Phys. Lett. B **761**, 456 (2016).
33. J. Haidenbauer, U.-G. Meißner and L. Y. Dai, Phys. Rev. D **103**, 014028 (2021).
34. A. I. Milstein and S. G. Salnikov, Phys. Rev. D **105**, L031501 (2022).
35. J. Haidenbauer and U.-G. Meißner, Eur. Phys. J. A **59**, 136 (2023).



- 
36. S. G. Salnikov and A. I. Milstein, JETP Lett. **117**, 905 (2023)
  37. M. Ablikim *et al.* [BES], Phys. Rev. Lett. **93**, 112002 (2004).
  38. M. Ablikim *et al.* [BESIII], Phys. Rev. D **87**, 012007 (2013).
  39. M. Ablikim *et al.* [BESIII], Phys. Rev. D **100**, 052010 (2019).
  40. M. Ablikim *et al.* [BESIII], Phys. Rev. Lett. **131**, 151901 (2023).
  41. M. Ablikim *et al.* [BES], Phys. Lett. B **659**, 789 (2008).
  42. M. Ablikim *et al.* [BESIII], JHEP **11**, 217 (2021).
  43. H. Li *et al.* [GlueX], AIP Conf. Proc. **2249**, 030037 (2020).
  44. P. Pauli [GlueX], EPJ Web Conf. **271**, 02001 (2022).
  45. M. Z. Wang *et al.* [Belle], Phys. Rev. Lett. **90**, 201802 (2003).
  46. B. Aubert *et al.* [BaBar], Phys. Rev. D **79**, 112009 (2009).
  47. Q. L. Xie *et al.* [Belle], Phys. Rev. D **72**, 051105 (2005)
  48. R. Aaij *et al.* [LHCb], Phys. Rev. Lett. **131**, 031901 (2023).
  49. A. M. Sirunyan *et al.* [CMS], JHEP **12**, 100 (2019).
  50. E. Klempt, F. Bradamante, A. Martin and J. M. Richard, Phys. Rept. **368**, 119 (2002).
  51. J. Haidenbauer, T. Hippchen, K. Holinde, B. Holzenkamp, V. Mull and J. Speth, Phys. Rev. C **45**, 931 (1992).
  52. J. Haidenbauer, K. Holinde, V. Mull and J. Speth, Phys. Rev. C **46**, 2158 (1992).
  53. J. Adams *et al.* [STAR], Phys. Rev. C **74**, 064906 (2006).
  54. A. Kisiel, H. Zbroszczyk and M. Szymański, Phys. Rev. C **89**, 054916 (2014).
  55. S. Acharya *et al.* [ALICE], Phys. Lett. B **802**, 135223 (2020).
  56. S. Acharya *et al.* [ALICE], Phys. Lett. B **829**, 137060 (2022).
  57. E. Byckling and K. Kajantie, Particle Kinematics, John Wiley and Sons (1973).
  58. H. Huang, J. Ping and F. Wang, Mod. Phys. Lett. A **27**, 1250039 (2012).
  59. M. Ablikim *et al.* [BESIII], [arXiv:2401.09012 [hep-ex]].
  60. H. Machner, J. Haidenbauer, F. Hinterberger, A. Magiera, J. A. Niskanen, J. Ritman and R. Siudak, Nucl. Phys. A **901**, 65 (2013).
  61. S. Acharya *et al.* [ALICE], Phys. Lett. B **833**, 137272 (2022).
  62. G. Y. Wang, M. Y. Duan, E. Wang and D. M. Li, Phys. Rev. D **102**, 036003 (2020).